







Article

Glycosyl Mobile Radical Structures of Folic Acid Receptors Impact the Internalization of Functionalized Folate Amphiphilic Alternating Copolymer in Cancer Cells

Emilyn B. Aucoin ^{1,†} , Elizabeth Skapinker ^{2,†}, Abdulrahman M. Yaish ³ , Yunfan Li ², Haley L. Kombargi ³ , Daniel Jeyaraj ³ , Pankaj Garg ^{4,5} , Nicole Mendonza ⁶, Cecile Malardier-Jugroot ^{6,*} and Myron R. Szewczuk ^{4,*} 

¹ Faculty of Science, Biology (Biomedical Science), York University, Toronto, ON M3J 1P3, Canada; emilynaucoin@gmail.com

² Faculty of Arts and Science, Queen's University, Kingston, ON K7L 3N9, Canada; 21ess18@queensu.ca (E.S.); 18yl210@queensu.ca (Y.L.)

³ Faculty of Health Sciences, Queen's University, Kingston, ON K7L 3N9, Canada; a.yaish@queensu.ca (A.M.Y.); 20h1k@queensu.ca (H.L.K.); 19dj20@queensu.ca (D.J.)

⁴ Department of Biomedical & Molecular Sciences, Queen's University, Kingston, ON K7L3N6, Canada; pankaj.garg@univ-tlse3.fr

⁵ Toulouse Graduate School of Cancer Ageing and Rejuvenation (CARE), Université Toulouse III-Paul Sabatier, 31400 Toulouse, France

⁶ Department of Chemistry and Chemical Engineering, Royal Military College of Canada, Kingston, ON K7K 7B4, Canada; nicole.mendonza@queensu.ca

* Correspondence: cecile.malardier-jugroot@rmc.ca (C.M.-J.); szewczuk@queensu.ca (M.R.S.)

† These authors contributed equally to this work.

Simple Summary: Smart, multifunctional nanoparticles (NPs) combine targeting strategies to overcome barriers and increase the efficacy of drug delivery. They can encapsulate anti-cancer therapeutic drugs, possess a targeting mechanism to locate malignant tissue effectively, and respond to stimuli releasing its cargo. The properties of these smart NPs ensure that the therapeutic drugs are not released before reaching target tissues and are only released at a specific rate to provide the most potent and sustained effect. Here, we designed and fabricated a functionalized folic acid (FA) conjugated poly(styrene-*alt*-maleic anhydride) (SMA) via biological linker 2,4-diaminobutyric acid (DABA) (FA-DABA-SMA) copolymer. The empty FA-DABA-SMA interactions with folic acid receptors (FR α) have been reported to disrupt intracellular signaling processes by dysregulating FR α , resulting in a secondary therapeutic mechanism of action. This process depends on the size and shape of the FA-DABA-SMA. In this study, we investigated if the FR α glycosylation profiles impact the FA-DABA-SMA binding and internalization of pancreatic PANC-1 cancer cells.

Abstract: Folate receptor alpha (FR α) is a glycosylphosphatidylinositol (GPI) membrane-anchored protein containing three N-glycosylated residues at the N47, N139, and N179 termini. These glycosylation sites have been reported to be crucial for the receptor's structural integrity and its ability to bind and internalize FA. Here, we investigated the role of FR α glycosylation in the binding and internalization efficacy of FA-DABA-SMA in pancreatic PANC-1 cancer cells. There is a strong association of the FA copolymer with FR α with a Pearson coefficient R-value of 0.7179. PANC-1 cancer cells were pretreated with *maackia amurensis* lectin II (MAL-2), *sambucus Nigra* lectin (SNA-1), peanut agglutinin (PNA), and wheat germ agglutinin lectin (WGA) at different doses followed by 20 kDa and 350 kDa FA-DABA-SMA loaded with coumarin 153 (C153). Increasing the dosage of MAL2, SNA-1, PNA, and WGA concomitantly and significantly increased the internalization of C153-loaded FA-DABA-SMA in the cells. The half maximal effective lectin concentrations (EC50) to induce cellular internalization into the cytoplasm of the lectins for MAL-2 were 35.88 μ g/mL, 3.051 μ g/mL for SNA-1, 7.883 μ g/mL for PNA, and 0.898 μ g/mL for WGA. Live cell imaging of the internalization of 20 kDa and 350 kDa FA copolymers indicated an aggregation of 350 kDa copolymer with FR α in the cytoplasm. In contrast, the 20 kDa FA copolymer remained in the membrane. The data indicate for the first time that the mobile positions of the glycosyl radical groups and the



Citation: Aucoin, E.B.; Skapinker, E.; Yaish, A.M.; Li, Y.; Kombargi, H.L.; Jeyaraj, D.; Garg, P.; Mendonza, N.; Malardier-Jugroot, C.; Szewczuk, M.R. Glycosyl Mobile Radical Structures of Folic Acid Receptors Impact the Internalization of Functionalized Folate Amphiphilic Alternating Copolymer in Cancer Cells. *Receptors* **2024**, *3*, 457–473. <https://doi.org/10.3390/receptors3040023>

Academic Editor: Stephen H. Safe

Received: 18 August 2024

Revised: 8 October 2024

Accepted: 17 October 2024

Published: 21 October 2024



Copyright: © 2024 by the authors. Licensee MDPI, Basel, Switzerland. This article is an open access article distributed under the terms and conditions of the Creative Commons Attribution (CC BY) license (<https://creativecommons.org/licenses/by/4.0/>).

receptor tilt in generating steric hindrance impacted the individual FR α receptors in the binding and internalization of 350 kDa FA–DABA–SMA in cancer cells.

Keywords: folate receptor alpha (FR α); glycosylation; functionalized folic acid (FA)-conjugated copolymer; lectins; pancreatic cancer cells

1. Introduction

Folate receptor alpha (FR α) is a glycosylphosphatidylinositol (GPI) membrane-anchored protein that promotes efficient endocytic uptake of folic acid (FA) from the luminal surface of epithelial and cancer cells [1]. FA, commonly known as vitamin B₉, is a one-carbon donor required to produce vital components of nucleic acids, such as thymidine and purines [2]. As a result, the binding of FA to the FR α receptor facilitates various essential cellular metabolic activities, including DNA, RNA, and amino acid synthesis [3].

Interestingly, FR α expression is typically restricted in normal cells [3]. However, studies have revealed that FR α is overexpressed in rapidly proliferating cells, as these cells require higher levels of FA to support their heightened metabolic demands [3]. This upregulation of FR α is especially notable in solid tumors ranging from ovarian and breast cancers to pancreatic carcinomas [4]. In fact, it is estimated that 40% of human cancers are associated with an overexpression of FR α , leading to clinically significant increases in tumor aggression [4]. Hence, by exploiting this overexpression, numerous targeted therapies have been developed to achieve adequate selectivity and efficacy while mitigating off-target toxicity.

FR α is a logical target for NP-based cancer therapies for several reasons. First, the small, non-immunogenic, and globular structure of FR α enhances its ability to bind and internalize FA after conjugation with another drug or biomarker [5]. Thus, conjugation of FA via the biodegradable linker DABA, the FA–DABA–SMA copolymer, was found to exhibit precise active targeting (i.e., a directing moiety to increase selective toxicity toward the target cell) [6]. These FA–DABA–SMA copolymers are composed of functionalized folic acid (FA) linked via a biodegradable linker, 2,4-diaminobutyric acid (DABA), to an amphiphilic alternating copolymer, poly(styrene-*alt*-maleic anhydride) (SMA) [7,8]. These nanostructures of the FA–DABA–SMA self-assemble at pH 7 to encapsulate hydrophobic drugs in their interior core and are responsive to pH changes [9,10]. Once bound to the FR α expressed on cancer cells, it is internalized via an endocytic pathway [7,9]. This internalization subjects the FA–DABA–SMA to an acidic environment (pH 5), which causes a conformational change that deposits the therapeutic load into the cell [10]. Sambi et al. [11] have also reported that both the 20 kDa and the 350 kDa FA–DABA–SMA copolymer target FR α on the cell surface, triggering the internalization of the copolymer to the cell's cytoplasmic interior. The 350 kDa copolymer with a hydrodynamic radius (Rh) of 6 nm self-assembles into sheets. The smaller 20 kDa copolymer with an Rh of 3 nm self-assembles into cylinders. Additionally, each size of the copolymer's fabrication had a density of one FA for every 10 SMA monomers within the chain [12].

Interestingly, the 350 kDa copolymer has been reported to turn off cell division through disruptions of essential oncogenes such as p53, STAT-3, and c-Myc; however, the 20 kDa copolymer did not [11]. These results suggested that the size and the sheet shape of the 350 kDa FA–DABA–SMA play a significant role in the initiation of multimodal tumor targeting mechanisms that shut down oncogenes that control cell division. In addition, the 350 kDa copolymer has been reported to impact multicellular pancreatic tumor spheroids and breast tumor spheroids [8]. Interestingly, the empty 350 kDa copolymers were able to decrease the spheroid volume after 48 and 72 h. These intracellular disruptions may be due to the FA–DABA–SMA immobilizing FR α intracellular and dysregulating downstream cellular signaling [13].

Chen et al. [1] reported that human FR α contains three N-glycosylated residues at the N47, N139, and N179 termini. These glycosylation sites were found to be crucial for the receptor's structural integrity and functional features, as well as its ability to bind and internalize FA, as shown in numerous other studies [14]. Interestingly, an atomistic molecular dynamics study of FR α demonstrated that the structure and short-term dynamics of FR α under three different pressure scaling schemes demonstrated that the glycosyl groups are highly mobile [15]. The protein tilt (the angle closed between the protein's principal axis and the membrane's XY-plane) is highly variable but was found not to affect the accessibility of the binding pocket significantly [15].

To this end, we investigated the glycosyl mobile radical structures positions of FR α receptors and the FR α tilt in generating steric hindrance, which would impact the individual FR α receptors in the binding and internalization of the functionalized 350 kDa FA–DABA–SMA in cancer cells.

2. Materials and Methods

2.1. Cell Lines

PANC-1 (ATCC[®] CRL-1469[™]) from American Type Culture Collection (ATCC, Manassas, VA, USA) is a cell line originating from a pancreatic tumor of ductal cell origin from a 56-year-old white male. The cells were cultured in 1× Dulbecco's Modified Eagle Medium (DMEM), supplemented with 10% fetal bovine serum (FBS; HyClone, Logan, UT, USA) and 0.5 µg/mL plasmocin (InvivoGen, San Diego, CA, USA). All cells in the culture were incubated at 37 °C in a 5% CO₂ incubator.

2.2. Reagents

Coumarin 153 (C153; C₁₆H₁₄F₃NO₂) (Excision BioTherapeutics, Inc., 134 Coolidge Avenue, Watertown, MA, USA) belongs to the class of 7-aminocoumarins and functions as a fluorochrome. A total of 1 mg of C153 powder was added to the FA–DABA–SEM nanoparticles (NP) via physical entrapment and agitated overnight using a rocker plate to facilitate complete entrapment. Any excess undissolved C153 was removed by centrifugation, and the supernatant of C153-loaded FA–DABA–SMA was used for further studies.

Maackia amurensis lectin 2 (MAL-2) (Sigma Inc., L-0825) binds to α -2,3 sialic acid linked to terminal β -galactose. *Sambucus nigra* lectin 1 (SNA1; Bioworld, L-17071701) binds to α -2,6 sialic acid linked to terminal β -galactose and to a lesser degree α -2,3 sialic acid linkage; peanut agglutinin (PNA; Vector, galactosyl (β -1,3) N-acetyl galactosamine) and succinylated wheat germ agglutinin (sWGA; Vector, N-acetylglucosamine residues) were used in these studies.

2.3. FA–DABA–SMA Alternating Copolymer

A functionalized folic acid (FA) conjugated to poly(styrene-*alt*-maleic anhydride) (SMA) linked via a 2,4 diaminobutyric acid (DABA) biological linker (FA–DABA–SMA) copolymer was synthesized and characterized by us [9]. This copolymer is composed of alternating hydrophobic (styrene) and hydrophilic groups (maleic acid) along the SMA chain [9]. Two variations of the FA–DABA–SMA (NP) were used in this study to test the effects of size and shape. The large NP has an MW of 350,000 g/mol (350 kDa) with a hydrodynamic radius (Rh) of 1000 nm and self-assembles into sheets. The small NP has an MW of 20,000 g/mol (20 kDa) and an Rh of 120 nm, and it self-assembles into cylinders. Additionally, each size of the NP's fabrication had a density of one FA for every 10 SMA monomers on the chain.

2.4. Lectin Treatment

PANC-1 cells were plated onto circular 12 mm coverslips in a 24-well tissue plate (Becton Dickinson) at a density of approximately 15,000 cells per well and incubated for 24 h in 5% CO₂ at 37 °C. After removing media, lectins were introduced at various indicated concentrations in 1× DMEM medium along with an untreated control group

for 35 min. The lectin-treated cells were washed once with 1× phosphate-buffered saline (1× PBS) solution at pH 7.4, followed by 1:1000 dilution of Invitrogen CellMask™ Deep Red plasma membrane stain in 1× PBS solution at 37 °C for 7 min. The stained cells were washed three times with 1× PBS and treated with various dilutions of 350 kDa and 20 kDa C153-loaded FA–DABA–SMA, including a control for unloaded nanoparticles (NPs). After a 1 h incubation, the cells were washed three times with 1× PBS, and coverslips were inverted onto a fluorescence mounting media droplet. Pictures were taken with a ZEISS Axio Imager M2 fluorescent microscope (Carl Zeiss AG, Oberkochen, Germany) at 20× or 40× magnification at the respective time points using selective color channels.

The relative fluorescence density was assessed using two representative images taken at 40× magnification. Pixel measurements, background fluorescence (i.e., the unstained background), and mean fluorescence (i.e., total image fluorescence) were analyzed with Corel Photo-Paint X8. These measurements are subsequently utilized to determine the relative fluorescence density using the following formula:

$$\text{Relative fluorescent density} = (\text{bkg mean} - \text{mean}) \times \text{pixels}$$

2.5. C153-Loaded FA–DABA–SMA Copolymer Colocalizes with FR α

PANC-1 cells were cultured in a 1× DMEM medium with 10% FCS and 0.1% plasmocin. Cells were treated with 350 kDa C153-loaded FA–DABA–SMA Copolymer for 60 min or left untreated as controls. Cells were fixed, permeabilized, and immunostained with mouse monoclonal IgG anti-hFOLR1 (Lot # MAB5646, R&D Systems, Inc., Minneapolis, MN, USA) followed with goat anti-mouse conjugated with Alexa Fluor594 (Invitrogen, Life Technologies Inc., Eugene, OR, USA). Stained cells were visualized using a Zeiss M2 fluorescent microscope imager with a 20× or 40× objective. To calculate the percentage of colocalization in the selected images, the Pearson correlation coefficient was measured on a total of cells per image using Zeiss M2 fluorescent microscope software (Carl Zeiss™ AxioVision Rel. 4.8.2) and expressed as Pearson coefficient R-value. A correlation coefficient of 0.7 or greater indicates a strong positive correlation between two variables.

2.6. Live Cell Microscopy

Live cell microscopy imaging was conducted utilizing an inverted microscope (Leica DMi8) fitted with a high-speed camera from Photron Fastcam SA-Z with 100× oil objectives to visualize the stained live cell. PANC-1 cells (50,000 cells each) were seeded onto a 35 mm MatTek dish (MatTek Headquarters, 200 Homer Ave, Ashland, MA, USA) with a No. 1.5 gridded coverslip (14 mm glass diameter) in culture media containing 10% fetal calf serum. The cells were incubated for 24 h and left untreated. Live cells were washed with 1× PBS and then incubated with a 1:1000 dilution of Invitrogen CellMask™ Deep Red plasma membrane stain in 1× PBS solution at 37 °C for 7 min, followed by three washes with 1× PBS. The cells were treated with various dilutions of 20 kDa and 350 kDa C153-loaded FA–DABA–SMA. After a 1 h incubation, the cells were washed three times with 1× PBS. The dynamic colocalization of Invitrogen CellMask™ Deep Red plasma membrane stain (red) and C-153-loaded FA–DABA–SMA (green) was captured at one-second intervals and recorded as a video.

2.7. Statistical Analysis

Data are presented as the mean \pm the standard error of the mean (SEM) from at least seven independent experiments, each performed in septuplicate (n = 7). GraphPad Prism ver.10.2.2. was used for data visualization and statistical analysis. Differences between groups subjected to lectin treatment and control groups from seven independent experiments were assessed using a one-way analysis of variance (ANOVA) using the uncorrected Fisher's least significant difference (LSD) test at a 95% confidence level. Statistical significance was considered at $p < 0.05$, indicated by asterisks.

3. Results

3.1. Concentration Dependence of Lectins MAL-2, SNA-1, PNA, and WGA Effect on the Internalization of FA–DABA–SMA Copolymer in PANC-1 Cancer Cells

Hülsmeier et al. [14] have reported that FR α glycosylation sites are involved not only in the structural integrity of the receptor but also in their ability to bind and internalize FA. Here, we hypothesized that these glycosylated sites of FR α expressed on cancer cells may also play a role in the binding and internalization of functionalized FA–DABA–SMA copolymer. In support of this premise, Amith et al. [16] have reported that lectin binding to α -2,3-sialyl residues enables Toll-like receptor (TLR) dimerization by removing a steric hindrance to receptor association and the subsequent recruitment of MyD88 to the receptor. The removal of these residues by Neu1 sialidase activity facilitated TLR dimerization, MyD88/TLR complex formation, and subsequent NF κ B activation [16]. Here, we examined whether the addition of lectins, which specifically bind to different glycosylation sites on FR α on the surface of PANC-1 cancer cells, would impact the binding and internalization of the FA–DABA–SMA copolymer.

The lectins used in these studies are *Maackia amurensis* lectin II (MAL-2), *Sambucus nigra* lectin (SNA-1), peanut agglutinin (PNA), and wheat germ agglutinin lectin (WGA). MAL-2 is a hemagglutinating lectin that detects N-linked glycans and targets α 2-3-linked sialic acids [17]. The SNA-1 lectin detects α 2,6-linked sialic acids located on the surface of many cancer cells. It is often used as an effective diagnostic tool for various types of cancer as secretion of α 2,6-linked sialic acid has been associated with poor prognosis and decreased chance of disease survival [18]. The PNA lectin binds the T-antigen N-acetylgalactosamine structure present on glycoconjugates, gangliosides, and many membrane-associated glycoproteins and lipids [19]. When sialylated, it prevents receptor binding and is frequently used to measure the intake or prevention of entry of molecules into the cell. The WGA lectin binds preferentially trimers and dimers of the N-acetylglucosamine structures found on membrane-associated glycoproteins and lipids. It is used as an efficient tagging tool to determine the presence of N-acetylglucosamines in cells [20]. N-acetylglucosamines are linked to cancer cell proliferation and metastasis, making WGA lectins an excellent tool for tracking cancer growth [21].

The data depicted in Figure 1A demonstrate a concentration-dependence effect of MAL-2, SNA-1, PNA, and WGA on the internalization of the FA–DABA–SMA-loaded C-153 (NP-C153) copolymer in PANC-1 cells. Increasing the dose of MAL-2 (Figure 1B,C), SNA-1 (Figure 1D,E), PNA (Figure 1F,G), and WGA (Figure 1H,I) concomitantly significantly increased the internalization of C153-loaded FA–DABA–SMA in the cells. Interestingly, the half maximal effective concentration (EC₅₀) of lectins for MAL-2 is 35.88 μ g/mL (Figure 1C), 3.05 μ g/mL for SNA-1 (Figure 1E), 7.88 μ g/mL for PNA (Figure 1G), and 0.89 μ g/mL for WGA (Figure 1I) to induce cellular internalization into the cytoplasm as depicted in Figure 1 respectively with concomitant images (Figure 1I). The EC₅₀ values represent the concentration of the lectin that induces a response halfway between the baseline and maximum, indicating the potency of the effect on FA–DABA–SMA internalization.

3.2. MAL-2 Lectin Enhances the Internalization of C153-Loaded FA–DABA–SMA at Different Dilutions of the Copolymer

The data depicted in Figure 1A demonstrated a markedly significant internalization of the 350 kDa FA–DABA–SMA copolymer in the presence of 100 μ g/mL MAL-2. Here, we questioned whether the mobile positions of the glycosyl α -2,3-sialyl groups blocked by MAL-2 would alter the FR α tilt and steric hindrance, impacting the binding and internalization of the functionalized 350 kDa FA–DABA–SMA at different dilutions in the cancer cells. To explain this conceptual approach, Gocheva et al. [15] reported on the folic acid receptor in that the glycosylated amino acids of the receptor are quite mobile. Here, the rationale is that when neuraminidase-1 cleaves α 2-3-linked sialic acids, this enables the removal of a steric hindrance to receptor association, dimerization, and downstream signaling [16]. The folic acid receptor has a very high sialic acid content, which could result in a large

amount of steric hindrance. Here, we proposed that the binding of MAL-2 and SNA-1 lectins to these α 2-3-linked sialic acid residues on FR α reduced steric hindrance to allow accumulation of FR α binding to folic acid conjugated on the copolymer.

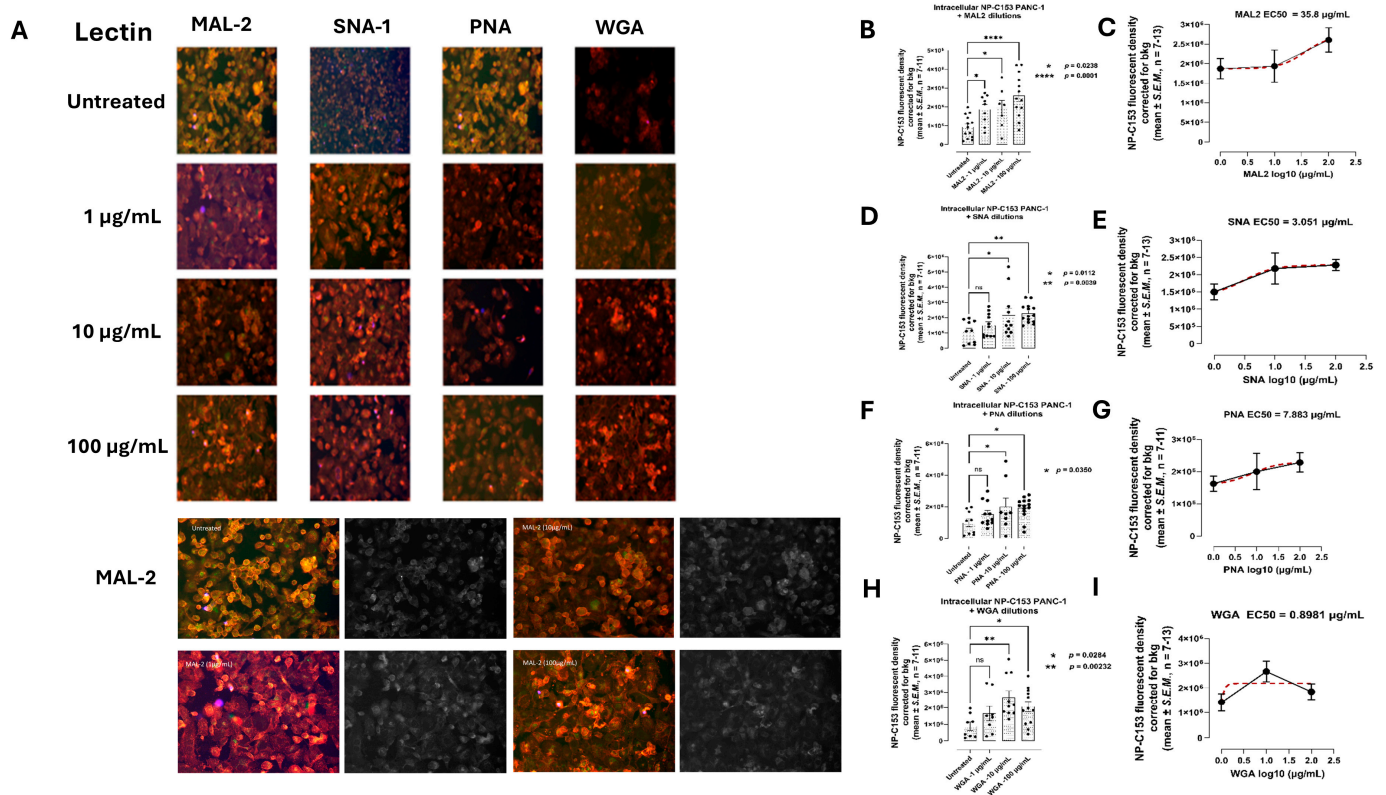


Figure 1. Concentration dependence of (A) MAL-2, SNA-1, PNA, WGA, and their half maximal effective concentration (EC50) of lectins (B,C) MAL-2, (D,E) SNA-1, (F,G) PNA, and (H,I) WGA to induce C153-loaded FA–DABA–SMA internalization into the cytoplasm of PANC-1 cells. Cells were plated in a 24-well plate and incubated overnight. Each lectin was added to wells at designated concentrations, and cells were incubated for 35 min and washed with 1× PBS. Coumarin 153 (C153; C16H14F3NO2) belongs to the class of 7-aminocoumarins and functions as a green fluorochrome. Cells were incubated in 150 µg/mL of CellMask™ Deep Red plasma membrane stain diluted 1:1000 in 1× PBS for 7 min and washed three times in 1× PBS. C153-loaded FA–DABA–SMA was added to wells, incubated for 1 h, and washed three more times with 1× PBS. Samples were mounted onto glass slides with Fluoroshield Mounting Medium and imaged using a ZEISS Axio Imager M2 fluorescent microscope (Carl Zeiss AG, Oberkochen, Germany) at 40× magnification. (B–I) The results were analyzed with Corel Photo-Paint X8 for background means, green C-153 stain image means, and pixel measurements. The results are depicted as scatter plots for visualization using dots to represent fluorescent density (n = 7–11). The mean fluorescent density corrected for background (bkg) + SEM is indicated for each concentration of lectin. The mean fluorescent density at each concentration of lectin was compared to the mean of the untreated cells by ANOVA using a Fisher’s LSD with 95% confidence. Statistical significance is indicated with asterisks. (C,E,G,I) The EC50 is defined as the concentration of agonist that results in a response that is halfway between the baseline and maximum response. This concentration is used to measure each lectin’s potency to induce internalization of the copolymer. The dashed red line is the calculated simple linear regression using the GraphPad Prism software (version 10.3.1.509).

When the cells were treated with 100 µg/mL of MAL-2, the internalization of the 350 kDa nanoparticle significantly increased at all of the indicated dilutions (Figure 2). It is noteworthy that at the 1/1 dilution of the nanoparticle, internalization was highest in the

presence of MAL-2, while internalization consistently decreased with increased dilutions of the nanoparticle with MAL-2.

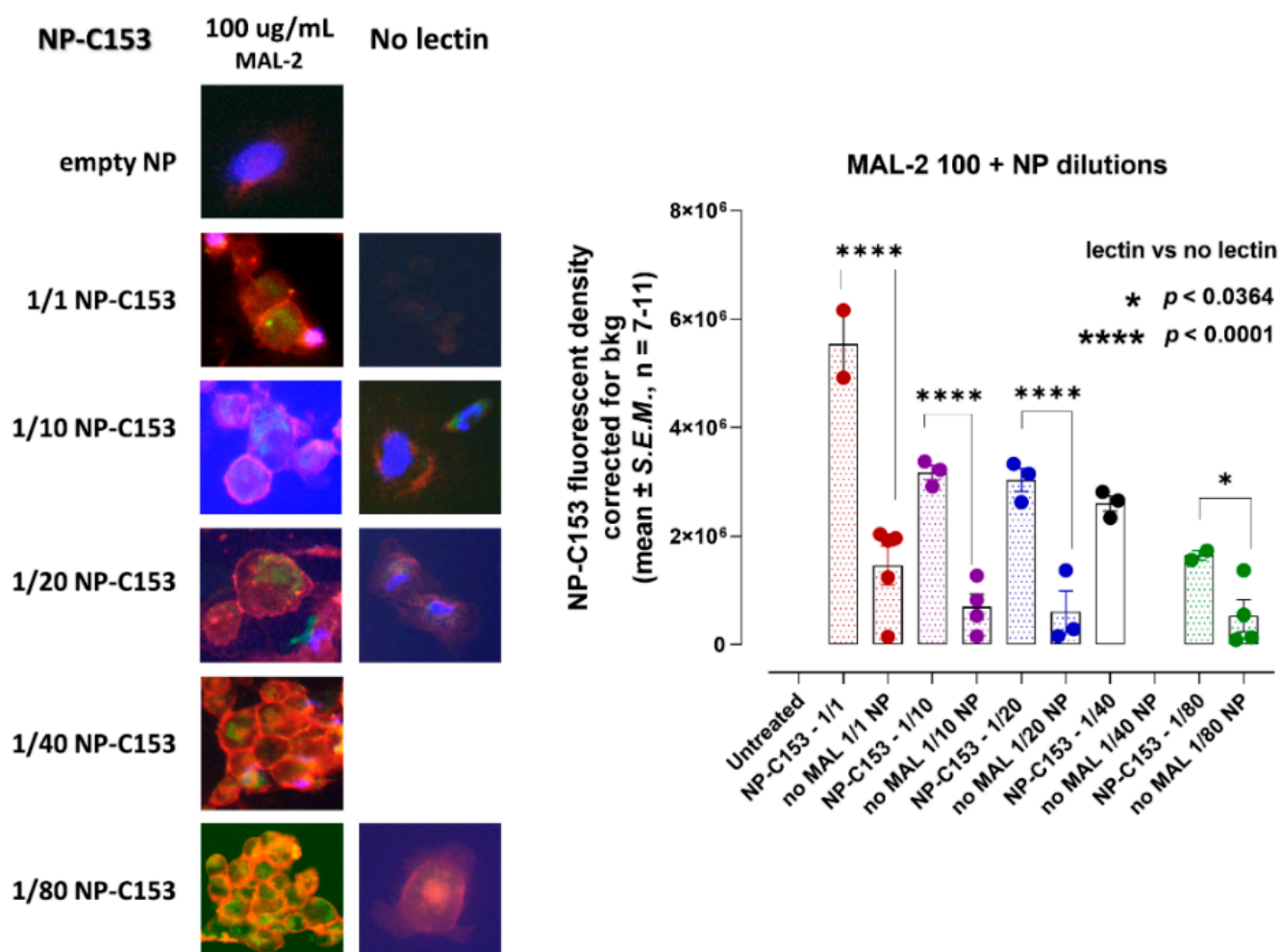


Figure 2. Evaluating the concentration dependence of coumarin-153-loaded FA-DABA-SMA (NP-C153) internalization into cells in the presence of 100 µg/mL MAL2 lectin. Cells were plated in a 24-well plate and incubated overnight. MAL-2 was added to wells, and the cells were incubated for 35 min. Then, they were washed with 1× PBS. Cells were incubated in 150 µg/mL of CellMask™ Deep Red plasma membrane stain diluted 1:1000 in 1× PBS for 7 min and washed three times in 1× PBS. C153-loaded FA-DABA-SMA was added to wells at different dilutions, incubated for 1 h, and washed three more times with 11× PBS. Samples were mounted onto glass slides with Fluoroshield Mounting Medium and imaged using a ZEISS Axio Imager M2 fluorescent microscope (Carl Zeiss AG, Oberkochen, Germany) at 40× magnification. The results were analyzed with Corel Photo-Paint X8 for background means, image means, and pixel measurements. The results are depicted as a bar graph for visualization of the mean intracellular NP-C153 fluorescent density corrected for background (bkg) ± SEM of varying dilutions of copolymer with and without MAL-2. The mean fluorescent density of each dilution without MAL-2 was compared to the mean fluorescent density of the same dilution with MAL-2 by ANOVA with a Fisher's LSD multiple comparisons test with 95% confidence. Asterisks indicate statistical significance. Abbreviations: NP-C153: C153-loaded FA-DABA-SMA; NP: nanoparticle; bkg: background; ns: not significant.

3.3. Kinetics of Internalization of C153-Loaded FA-DABA-SMA into PANC-1 Cells

Here, we evaluated the kinetic efficacy of 350 kDa C153-loaded FA-DABA-SMA copolymer binding to the plasma cell membrane of PANC-1 cells to initiate copolymer internalization (Figure 3). At 0 s, C153-loaded FA-DABA-SMA copolymers approached

the cell membranes. At 30 s, there was minimal binding, which consistently increased at 60, 90, and 120 s. These results demonstrate the kinetic efficacy of progressive binding of C153-loaded FA–DABA–SMA copolymers to PANC-1 membranes. As depicted in Figure 4A, the colocalization of C153-loaded FA–DABA–SMA copolymers shows clear binding to the cell membrane. To confirm the specific binding of the copolymer to FR α receptors expressed on the cell membrane, the data shown in Figure 4B validated the predicted association of C153-loaded FA–DABA–SMA copolymers and FR α , indicating the specific binding of the copolymer to these receptors expressed on the cell membrane. Here, we measured the Pearson correlation coefficient, which measures the strength of a linear association between two variables. A high Pearson R-value represents the best-fit correlation between the two variables, indicating a strong association.

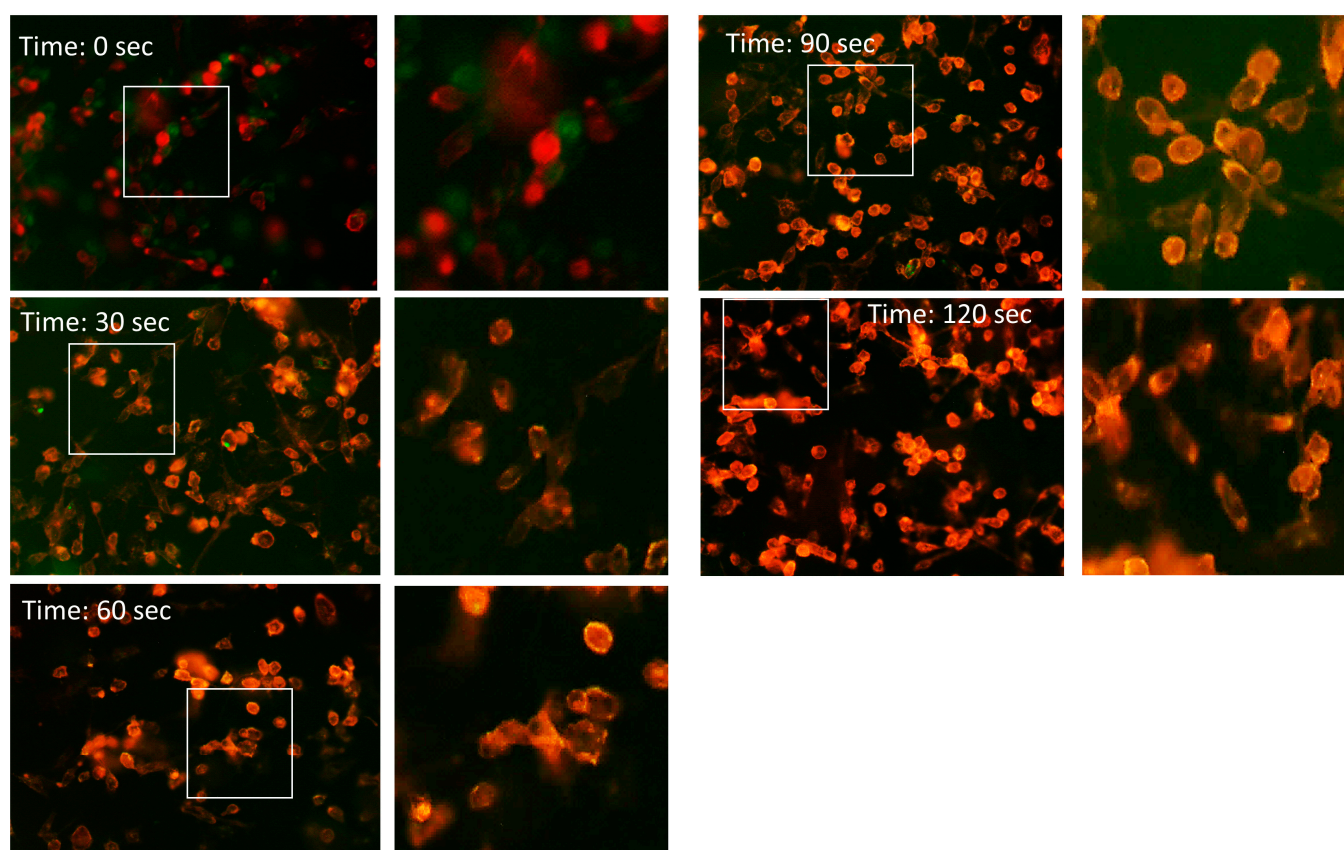


Figure 3. Kinetics of binding and internalization of C153-loaded FA–DABA–SMA into PANC-1 cells. Images in green depict fluorescence for C153-FA–DABA–SMA, and red fluorescence depicts CellMask™ Deep red plasma membrane stain. CellMask™ Deep Red, plasma membrane stain, diluted 1:1000 in 1× PBS, was added to cells at 150 μ L on circular glass slides in 24-well tissue culture dishes for 7 min and washed three times in 1× PBS. C153-FA–DABA–SMA copolymers were added to wells at indicated time points at 30, 60, 90, and 120 s and washed three times with 1× PBS. Cells on glass slides were mounted on microscope slides containing Fluoroshield Mounting Medium. Images were visualized using a ZEISS Axio Imager M2 fluorescent microscope (Carl Zeiss AG, Oerkochen, Germany) at 40 \times magnification.

To further support these observations, live cell microscopy and video expression of C153-loaded FA–DABA–SMA copolymers and cell membranes were assessed using an inverted Leica DMI8 fluorescent microscope equipped with a photron fastcam SA-Z high-speed camera (Figure 5). Live PANC-1 cells were cultured on a 35 mm Mattek dish, No. 1.5 gridded coverslip at 14 mm glass diameter in culture media containing 10% fetal calf serum for 24 h. Live cells were washed with 1× PBS and then incubated with a 1:1000 dilution of

Invitrogen CellMask™ Deep Red plasma membrane stain in $1\times$ PBS solution at $37\text{ }^{\circ}\text{C}$ for 7 min, followed by three washes with $1\times$ PBS. The cells were treated with 1/80 dilution of 20 kDa and 350 kDa C153-loaded FA–DABA–SMA. After a 1 h incubation, the cells were washed three times with $1\times$ PBS. The colocalization of Invitrogen CellMask™ Deep Red plasma membrane stain (red) and C-153-loaded FA–DABA–SMA (green) was captured at one-second intervals and recorded as a video. Live cell videos of PANC-1 are given in Supplementary Video S1 for Figure 5B,D.

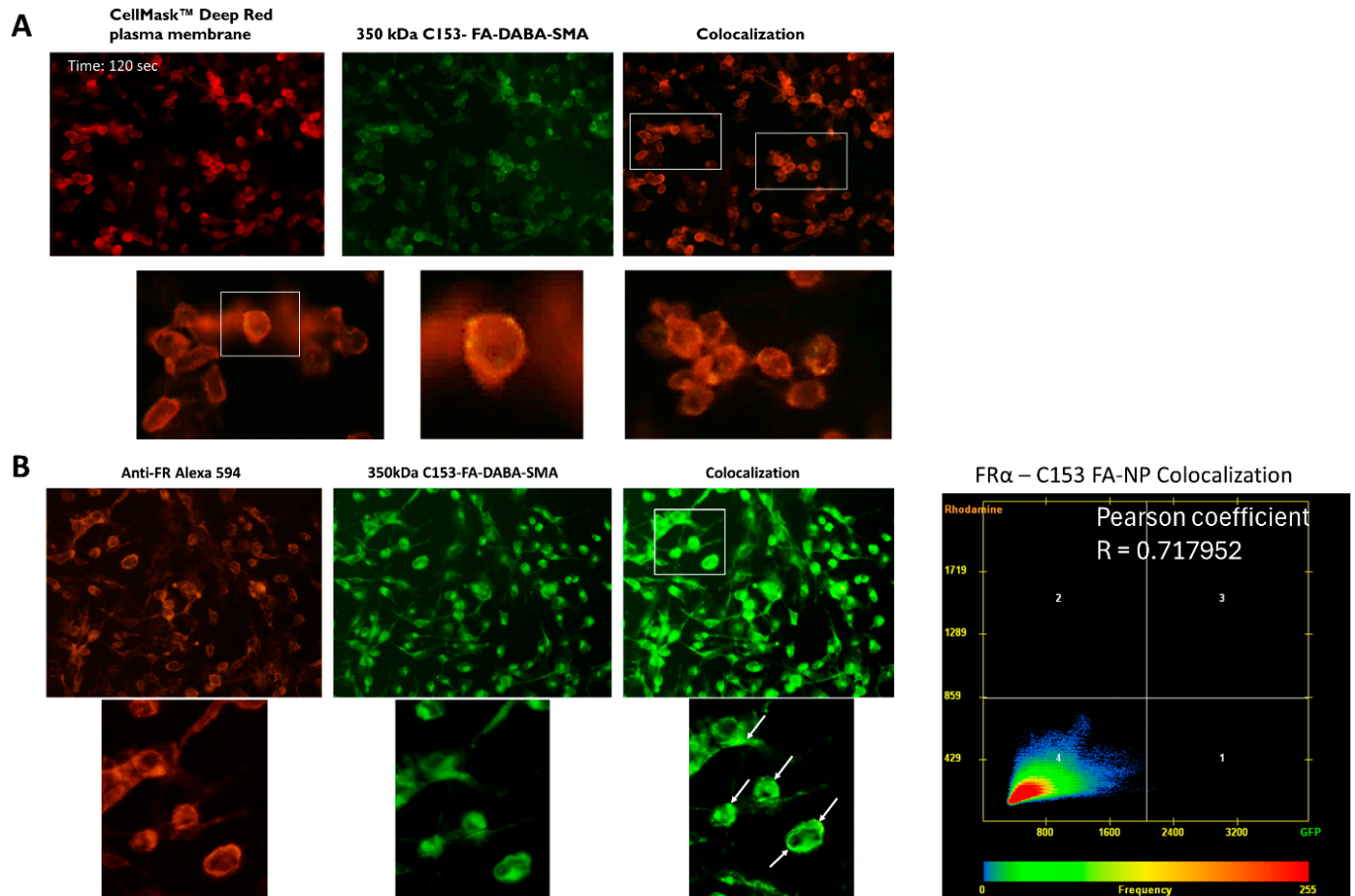


Figure 4. Colocalization of binding of C153-loaded FA–DABA–SMA to the (A) cell membrane and (B) the FR α receptor in PANC-1 cells. Images in green depict fluorescence for C153-FA–DABA–SMA, and red fluorescence depicts CellMask™ Deep red plasma membrane stain. Illustrated boxes signify the enlargement of the area for visualization. (A) CellMask™ Deep Red, plasma membrane stain, diluted 1:1000 in $1\times$ PBS, was added to cells at $150\text{ }\mu\text{L}$ on circular glass slides in 24-well tissue culture dishes for 7 min and washed three times in $1\times$ PBS. (B) Cells (50,000 cells) were plated on 12 mm circular glass slides in culture media containing 10% fetal calf sera for 24 h and treated with C153-loaded FA–DABA–SMA. Cells were fixed, permeabilized, and immunostained with mouse monoclonal IgG anti-hFOLR1, washed in $1\times$ PBS, and followed with goat anti-mouse conjugated with Alexa Fluor594. Stained cells were visualized using a Zeiss M2 imager fluorescent microscope with a $40\times$ objective. Arrows represent the yellow color of green (C153-FA–DABA–SMA) and red (anti-FR conjugated Alexa 594) colocalization. The Pearson correlation coefficient was measured on a total image of cells and expressed as the Pearson coefficient R-value, which was calculated using Zeiss M2 imager software (Carl Zeiss™ AxioVision Rel. 4.8.2). The data represent one of three independent experiments showing similar results.

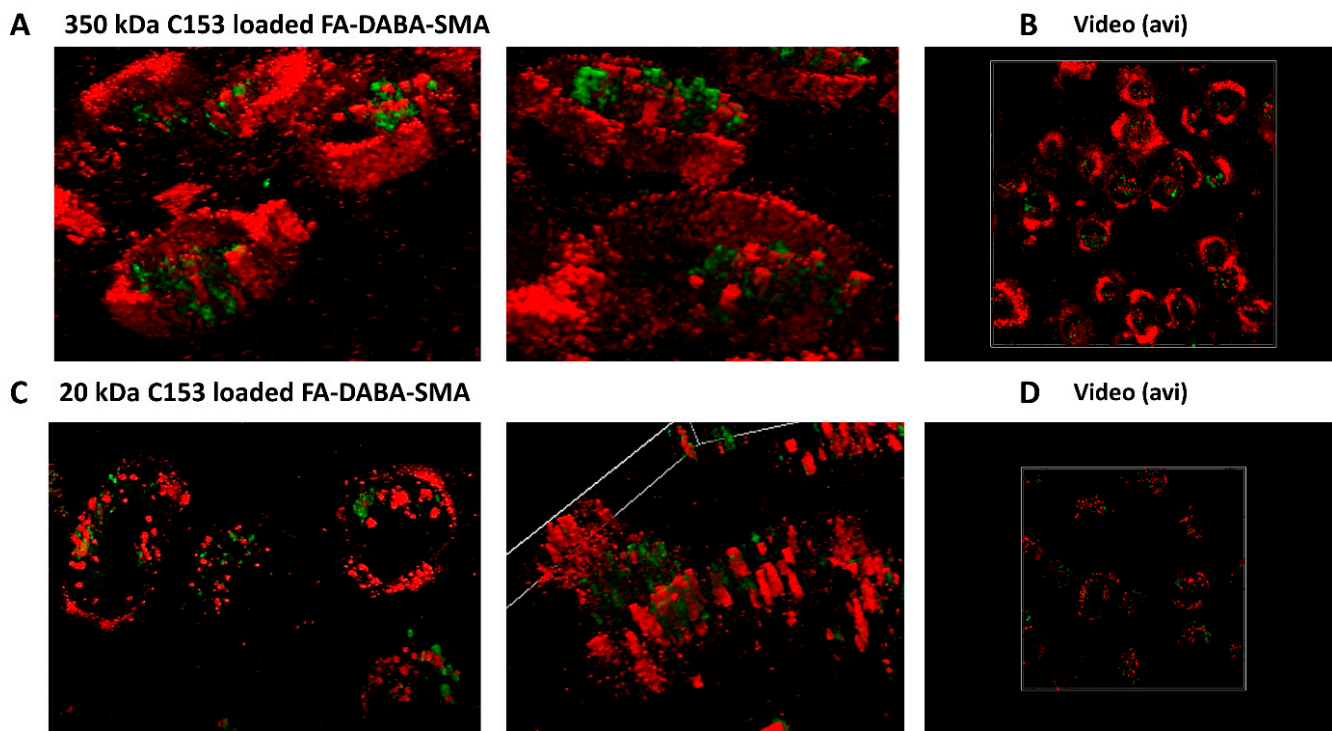


Figure 5. Live cell microscopy using an inverted microscope (Leica DMI8) equipped with a Photron Fastcam SA-Z high-speed camera. PANC-1 cells (50,000 cells) were plated on a 35 mm MatTek dish, No. 1.5 gridded coverslip at 14 mm glass diameter in culture media containing 10% fetal calf sera for 24 h and left untreated. Live cells were washed with $1\times$ PBS and incubated in 150 μ L of CellMask™ Deep Red plasma membrane stain diluted 1:1000 in $1\times$ PBS for 7 min and washed three times in $1\times$ PBS. (A) 350 kDa NP, (B) 350 kDa NP video, (C) 20 kDa NP, and (D) 20 kDa NP video of C153-loaded FA-DABA-SMA particles (green) were added to wells, then incubated for 1 h, and washed another three times with $1\times$ PBS. Samples were then mounted onto glass slides using Fluoroshield Mounting Medium. Images were visualized using a Leica DMI8 fitted with a high-speed camera from Photron Fastcam SA-Z with a $100\times$ oil objective. The kinetic expression of the cell membrane (red) and FA-DABA-SMA particles loaded with C153 (green) binding were taken every second and recorded as a Video S1 (B) for the 350 kDa copolymer and Video S2 (D) for the 20 kDa copolymer.

3.4. Lectins MAL-2, SNA-1, PNA, and WGA Effect on the Internalization Efficacy of 20 kDa and 350 kDa C153-Loaded FA-DABA-SMA into PANC-1 Cells

It is noteworthy that in Figure 5, both the 20 kDa and 350 kDa C153-loaded FA-DABA-SMAs bound to the cell membrane; however, the 20 kDa copolymer remained in the membrane while the 350 kDa copolymer massively internalized within the cell cytoplasm containing FR α /membrane-bound to the 350 kDa copolymer. Based on the data depicted in Figures 1 and 2, we asked if different concentrations of lectins MAL2, SNA-1, PNA, and WGA would impact the binding and internalization of 20 kDa C153-loaded FA-DABA-SMA compared with the 350 kDa copolymer.

The data depicted in Figure 6 indicate that the different lectins at the indicated concentrations did not affect the internalization of the 20 kDa C153-loaded FA-DABA-SMA copolymer compared with the 350 kDa copolymer. Notably, the 350 kDa copolymer, after treatment with 1, 10, and 100 μ g/mL of either MAL2, SNA-1, or PNA, showed significant internalization compared to the 20 kDa copolymer. In contrast, the lectin WGA induced a significantly higher internalization of the 20 kDa copolymer at 10 and 100 μ g/mL compared to the 350 kDa copolymer.

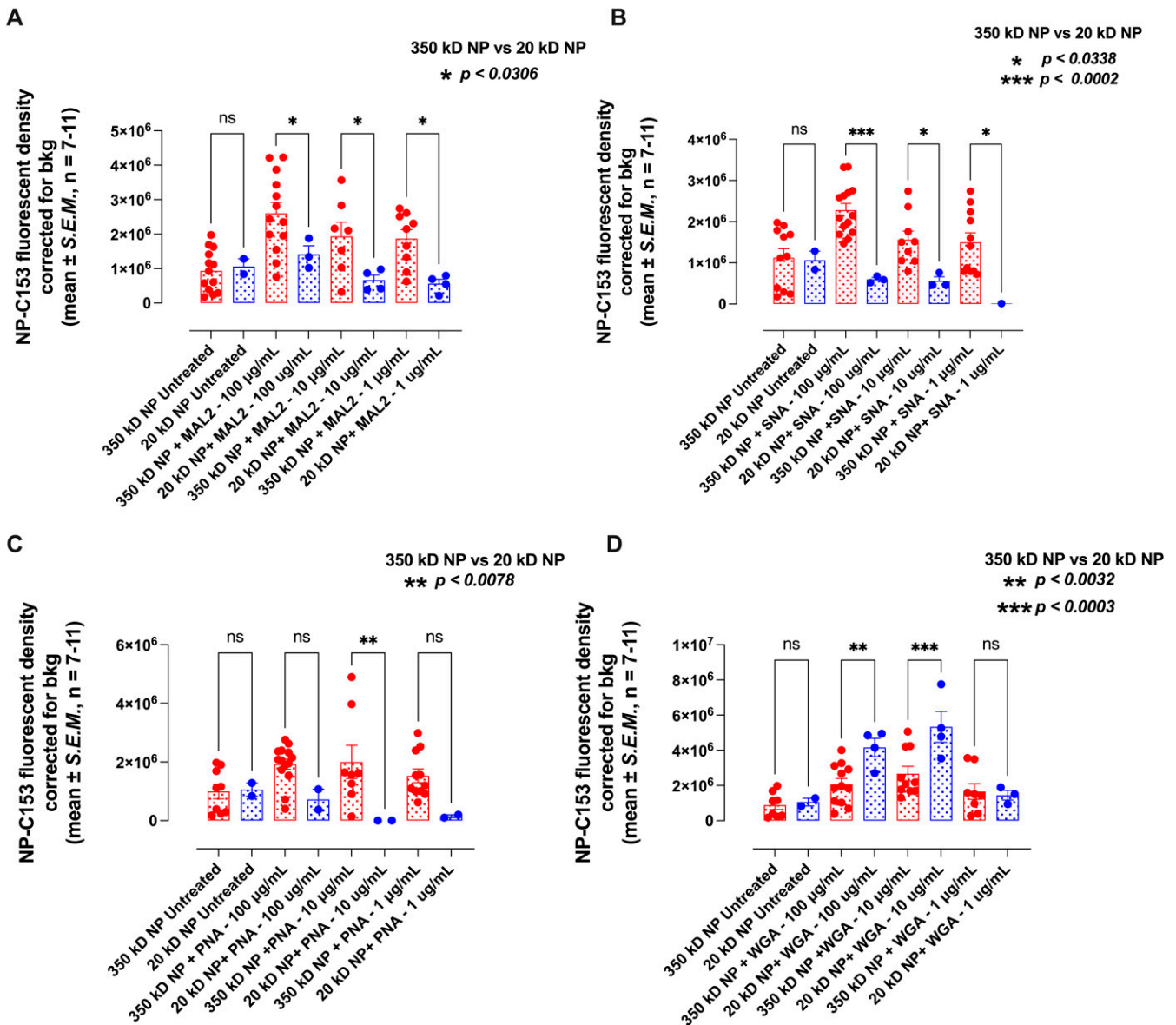


Figure 6. The efficacy of the internalization of the 350 kDa and 20 kDa C153-loaded FA–DABA–SMA NP into PANC-1 cells following treatment with (A) MAL2, (B) SNA-1, (C) PNA, and (D) WGA lectins at the indicated concentrations. PANC-1 cells were plated at a density of 100,000 to 200,00 cells/mL on glass coverslips in 24-well plates. Cells were treated with 200 µL of lectin at concentrations of 100 µg/mL, 10 µg/mL, and 1 µg/mL and incubated for 35 min. Cells were then washed with 1× PBS and incubated in CellMask™ Deep Red Plasma membrane stain and diluted to a concentration of 1:1000 in 1× PBS for 7 min. Cells were washed 3 times with 1× PBS and then treated with 170 µL of 20 kDa and 350 kDa C153-loaded FA–DABA–SMA per well and incubated for 1 h. Cells were subsequently washed with 1× PBS and mounted onto glass slides with Fluoroshield Mounting Medium. The images were visualized using a ZEISS Axio Imager M2 fluorescent microscope (Carl Zeiss AG, Oberkochen, Germany) at 40× magnification. The results are depicted as scatter bar graphs of the mean fluorescent density corrected for background luminescence ± SEM of 3 independent experiments performed in triplicates. The results of the treatments with 20 kDa and 350 kDa copolymers were compared using the one-way ANOVA Fisher (LSD) test comparisons with 95% confidence, indicated by asterisks for statistical significance. ns: not significant.

4. Discussion

The rationale of the present study was to determine the role of FR α glycosylation in the binding and internalization efficacy of C153-loaded FA–DABA–SMA copolymers in pancreatic PANC-1 cancer cells. The functionalized FA–DABA–SMA has been designed to bind to folate receptor alpha (FR α) expressed in cancer cells. Noteworthy, FR α is a glycosyl-phosphatidylinositol (GPI) membrane-anchored receptor containing three N-glycosylated residues at the N47, N139, and N179 termini of the receptor [1]. These glycosylation sites have been reported to be crucial for the receptor's structural integrity and functional features, as well as its ability to bind and internalize FA, as shown in numerous other studies [14].

To this end, we investigated whether the N-glycosylated residues expressed at the termini end of FR α receptors would impact the binding and internalization of C153-loaded FA–DABA–SMA copolymers into cancer cells. Here, we used *Maackia amurensis* lectin II (MAL-2) specific for N-linked glycans and targets α 2-3-linked sialic acids [17], *Sambucus nigra* lectin-1 (SNA-1) specific for α -2,6-linked sialic acids, peanut agglutinin (PNA) specific for T-antigen N-acetyl galactosamine structure, and wheat germ agglutinin lectin (WGA) specific for N-acetylglucosamine structures [20,21].

The data depicted in Figure 1 showed that at increased concentrations, the addition of lectins MAL-2, SNA-1, PNA, and WGA in combination with 350 kDa C153-FA–DABA–SMA copolymer increased the internalization of the copolymer. The half maximal effective concentration (EC50) of lectins for MAL-2 was 35.88 μ g/mL, 3.05 μ g/mL for SNA-1, 7.88 μ g/mL for PNA, and 0.89 μ g/mL for WGA to induce cellular internalization into the cytoplasm. When the cells were treated with 100 μ g/mL of MAL-2, the internalization of the 350 kDa nanoparticle significantly increased at all of the indicated dilutions (Figure 2). With the highest concentration of the nanoparticle, there was an increased internalization in the presence of MAL-2, with a consistent lower internalization and increased dilutions of the nanoparticle with MAL-2.

Notably, the human folic acid receptors isolated from a human placenta expressed 3 moles of sialic acid for each mole of receptor isolated [22]. Gocheva et al. [15] also reported that the glycosylated amino acids of the folic acid receptor are quite mobile. In addition, it has previously been reported that neuraminidase-1 cleaving α 2-3-linked sialic acids enabled the removal of a steric hindrance to receptor association, dimerization, and downstream signaling [23]. The folic acid receptor has a very high sialic acid content, which could result in a large amount of steric hindrance. Here, we proposed that the binding of MAL-2 and SNA-1 lectins to these α 2-3-linked sialic acid residues on FR α reduced steric hindrance to allow accumulation of FR α binding to folic acid conjugated on the copolymer. In this study, we used two variations of the NP to test the effects of size and shape. The large NP has an MW of 350,000 g/mol (350 kDa) with a hydrodynamic radius R_h (nm) of 1000 nm and self-assembles into sheets [9,13]. The small NP has an MW of 20,000 g/mol (20 kDa) with an R_h of 120 nm and self-assembles into cylinders (Figure 7). Additionally, each size of the NP's fabrication had a density of one FA for every 10 SMA monomers on the chain.

Using the PNA lectin, the data showed an increase in internalization of 350 kDa copolymer in the cell (Figure 1). To explain these data, it is important to highlight that PNA is known to bind galactose–galactosamine linkages preferentially but can also bind other galactose-containing carbohydrates [24] to which α 2-3-linked sialic acids are connected via galactosyl units by the α 2,3-linkage. A study by Antony et al. [22] reported 6 moles of galactose per mole of the isolated folic acid receptor. PNA lectin binding to these galactoses linked in close proximity with α 2-3-linked sialic acids was sufficient to remove steric hindrance of the FR α to bind to the copolymer. It is also possible that these galactose-containing carbohydrates create less steric hindrance in the FR α receptor compared to the terminal α 2-3 sialic acids.

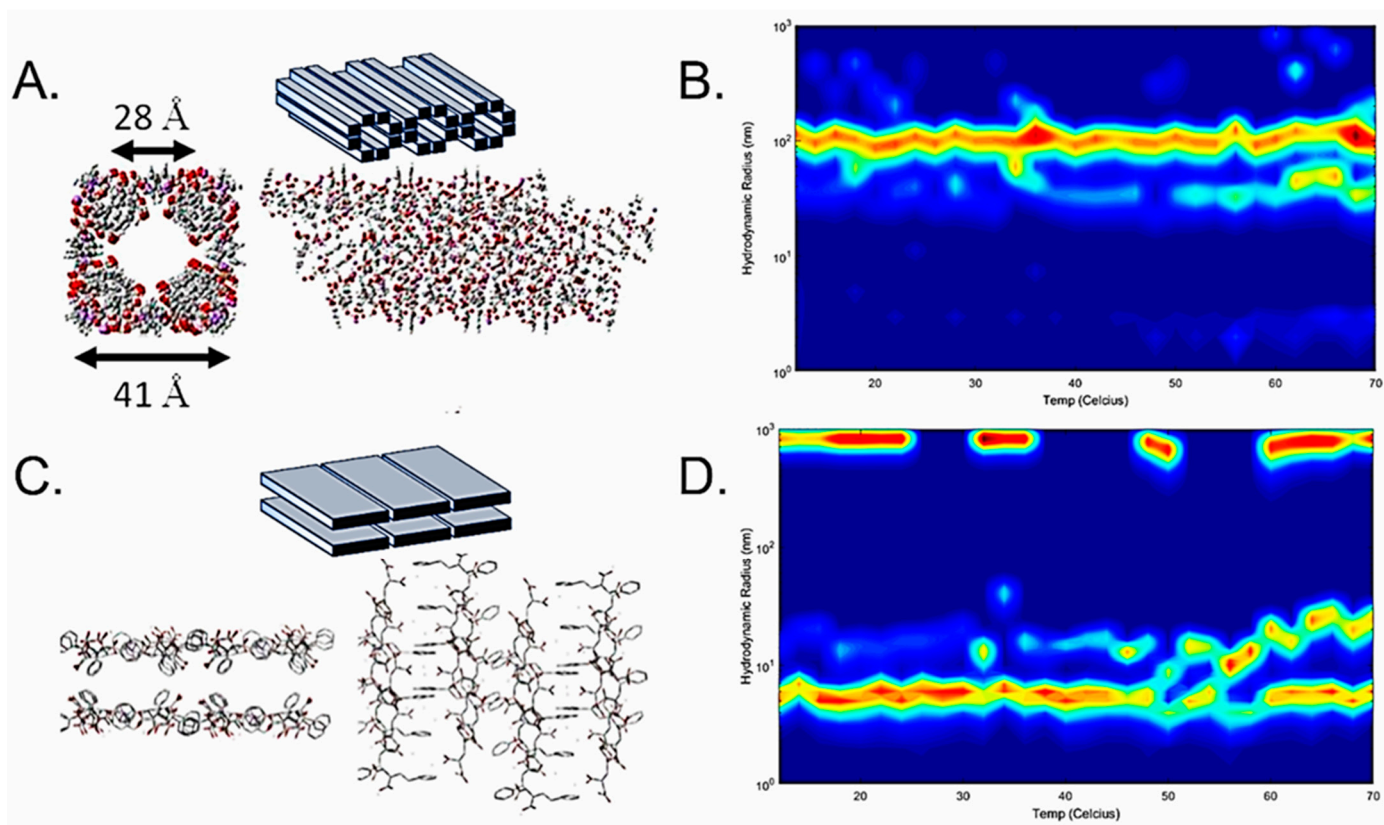


Figure 7. SMA in the nanotube and nanosheet configuration. (A) Schematic and molecular modeling representations of 20 kDa SMA self-assembly in neutral water. (B) Dynamic light scattering (DLS) spectrum of 20 kDa SMA in neutral water from 10 to 80 °C showing the stability of the structure with a ~100 nm hydrodynamic radius. (C) Schematic and molecular modeling representations of 350 kDa SMA self-assembly in neutral water. (D) DLS spectrum of 350 kDa SMA in neutral water from 10 to 80 °C showing the stability of the structure with a ~1000 nm hydrodynamic radius and unassociated SMA chains at ~10–20 nm. Images are adapted with permission of Taylor & Francis from Molecular Simulation, Characterization of a novel self-association of an alternating copolymer into nanotubes in solution, Malardier-Jugroot, C., van de Ven, T. G. M., and Whitehead, M. A., 31, 2–1, 2005; permission conveyed through Copyright Clearance Center, Inc. [12], and adapted from Chemical Physics Letters, 636, McTaggart, M., Malardier-Jugroot, C., and Jugroot, M., Self-assembled biomimetic nanoreactors I: polymeric template, 206–220, Copyright (2015), with permission from Elsevier [25] and by AIP Publishing (<https://doi.org/10.1063/5.0046081>, accessed on 15 August 2024).

The data depicted in Figure 1G showed that WGA also enhanced the internalization of the copolymer slightly less than SNA-1 but still more than PNA at 100 µg/mL. WGA is a homodimeric protein found in common bread wheat, and it binds to N-acetyl-D-glucosamine (GlcNAc) expressed on FR α [20]. Antony et al. [22] reported that the FR α receptor has 3 mol/mol of glucosamine. These glucosamine sites might also be involved in steric hindrance among the receptors on the cell membrane.

Also, WGA is the only lectin examined that increases the internalization of the 20 kDa copolymer compared to the 350 kDa copolymer. This occurs at both 100 µg/mL ($p = 0.0032$) and 10 µg/mL ($p = 0.0003$) (Figure 6D). These data depicted in Figure 6 indicate the efficacy of internalization of the 350 kDa and the 20 kDa C-I53-loaded FA–DABA–SMA nanoparticle for cells treated with MAL2, SNA-1, PNA, and WGA lectins at different concentrations. The results demonstrate that lectin treatment potentially enhances nanoparticle internalization compared to the control of no lectin. Notable, except for WGA, the 350 kDa nanoparticle is internalized far better than the 20 kDa copolymer with MAL2, SNA-1, and PNA lectins. Due to the mobility of the glycosyl groups located on the FR α , the receptors may generate

a form of steric hindrance that encourages the internalization of the 350 kDa nanoparticle with no effect on the internalization of the 20 kDa copolymer. Because of the small size and cylinder shape of the 20 kDa copolymer, WGA was the most effective lectin in internalizing the 20 kDa nanoparticle rather than the 350 kDa nanoparticle. It is likely that due to a conformational change in the binding pocket, the 20 kDa nanoparticle internalizes more effectively than the others.

As previously mentioned, WGA binds to N-acetyl-D-glucosamine (GlcNAc) on FR α . Figure 8 depicts a graphical representation of the FR α structure, including GlcNAc sites. The binding pocket (red) for folic acid is found inside multiple alpha-helices and is surrounded by GlcNAc at N47, N139, and N179 sites [1]. WGA contains a binding site that accounts for its specificity to GlcNAc and is responsible for interactions with sialic acid [20,26]. It has been previously reported that nanostructures conjugated with WGA can enhance internalization for drug delivery through receptor-mediated endocytosis [27]. This approach is achieved through its high affinity for GlcNAc and sialic acid residues on cell surface receptors. As seen in Figure 7, there is a GlcNAc glycosylation site, which is directly connected to a region of the binding pocket. We propose that WGA binding to this site would cause a conformational change in the binding pocket, which would result in the increased internalization of the 20 kDa FA–DABA–SMA observed. This conformational change could provide more flexibility within the pocket for FA to bind to the receptor. Due to the increased rigidity of the tubular conformation of the 20 kDa compared to the sheet conformation of the 350 kDa, the 350 kDa probably offers adaptability of the FA linked to the polymer for optimal binding with the FR α . Therefore, this optimal binding could be regained by a conformational change in the binding pocket. The proposed mechanism still requires elucidation; however, the data show a promising method for increasing the effectiveness of the internalization of these smaller nanostructures.

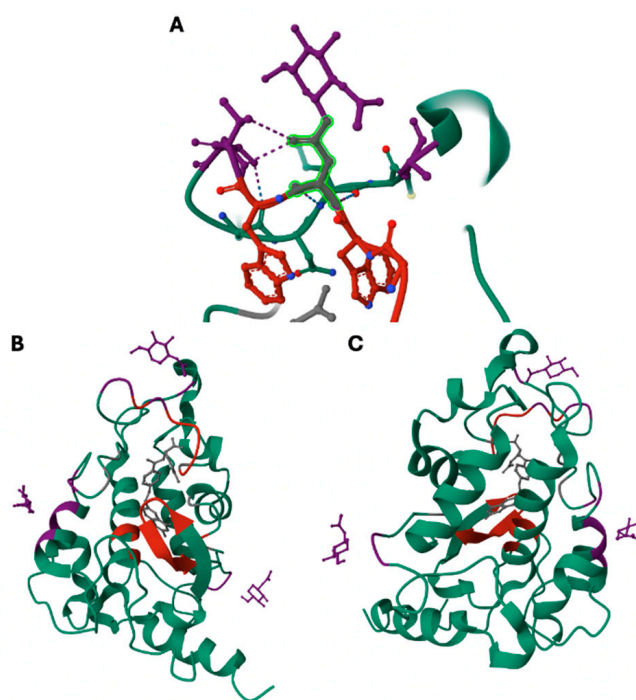


Figure 8. Graphical representation to visualize the structure of the folic acid receptor (FR α). Green structures depict amino acid chains for FR α , and N-acetyl-D-glucosamine (GlcNAc) sites are shown as purple projections from the amino acid chains. The folic acid binding pocket is labeled in red, and folic acid is labeled in grey. (A) The N139 glycosylation site, specifically with the bright green region highlighting the connection of this site to the binding pocket. At the same time, image (B) shows the

full structure of the folic acid receptor with the binding pocket exposed, and image (C) shows the structure rotated 180° relative to (B). Images adapted from the RCSB Protein Data Bank [<https://doi.org/10.2210/pdb4LRH/pdb>, accessed on 15 August 2024] are distributed under a CC0 1.0 Universal (CC0 1.0) Public Domain Dedication license [<https://creativecommons.org/publicdomain/zero/1.0/>, accessed on 15 August 2024] [1].

5. Conclusions

The human FR α contains critical N-glycosylated residues at the N47, N139, and N179 termini, which are crucial for the receptor's structural integrity and functional features as well as its ability to bind and internalize FA, as shown in other studies [14]. Gocheva et al. [15] proposed that the FR α receptor, using an atomistic molecular dynamics study, demonstrated that the structure and short-term dynamics of FR α under the glycosyl groups are highly mobile. The FR α tilt and the glycosyl mobile radical structures are proposed and supported by these data, which impacted the internalization of functionalized folate amphiphilic alternating copolymer in cancer cells.

Supplementary Materials: The following supporting information can be downloaded at: <https://www.mdpi.com/article/10.3390/receptors3040023/s1>, Video S1: Nano 20 1.avi; Video S2: Nano 350 1 20.avi.

Author Contributions: E.B.A., E.S., A.M.Y., Y.L., H.L.K., D.J., P.G., N.M., C.M.-J. and M.R.S. analyzed the literature, wrote, and read the manuscript. All authors made a significant contribution to the work reported, whether that is in the conception, study design, execution, acquisition of data, analysis, and interpretation, or all these areas; took part in drafting, revising, or critically reviewing the article; gave final approval of the version to be published; have agreed on the journal to which the article has been submitted; and agree to be accountable for all aspects of the work. All authors have read and agreed to the published version of the manuscript.

Funding: This work was supported by a grant to MRS from the Natural Sciences and Engineering Research Council of Canada (NSERC) Grant # RGPIN-2020-03869 and to CM-J from Canada Research Chair Program # 950-230272. The APC was funded by NSERC Grant # RGPIN 2020-3869.

Institutional Review Board Statement: Not applicable.

Informed Consent Statement: Not applicable.

Data Availability Statement: All data needed to evaluate the paper's conclusions are present. The preclinical datasets generated and analyzed during the current study are not publicly available but are available from the corresponding author upon reasonable request. The data will be provided following the review and approval of a research proposal, Statistical Analysis Plan, and execution of a Data Sharing Agreement. The data will be accessible for 12 months for approved requests, considering possible extensions; contact szewczuk@queensu.ca for more information on the process or to submit a request.

Acknowledgments: E.B.A. is the recipient of the York University Automatic Entrance Scholarship and the Faculty of Science Entrance Scholarship. A.M.Y. is the recipient of the 2023–2024 Advanced Placement scholarship. Y.L. is the recipient of the 2022–2023 Dean's Honour List, the E.D. Merkle Prize in Mathematics, and the M.C. Urquhart Book Prize in Economics. H.L.K. is the recipient of the Queen's University Principal's Scholarship, the Canadian Military Engineers Association Scholarship, and the Johnson's Scholarship. P.G. is the recipient of the 2024 Mitacs Globalink Research Internship. All authors have read and agreed to the published version of the manuscript. All authors acknowledge the educational and scholarly alliance of the Graduate Program in Experimental Medicine and the Health Sciences, HSCI BHSc Research, the Life Sciences program, and the Biomedical Science program at York University.

Conflicts of Interest: The authors declare no conflicts of interest.

References

1. Chen, C.; Ke, J.; Zhou, X.E.; Yi, W.; Brunzelle, J.S.; Li, J.; Yong, E.-L.; Xu, H.E.; Melcher, K. Structural basis for molecular recognition of folic acid by folate receptors. *Nature* **2013**, *500*, 486–489. [[CrossRef](#)] [[PubMed](#)]
2. Ducker, G.S.; Rabinowitz, J.D. One-Carbon Metabolism in Health and Disease. *Cell Metab.* **2017**, *25*, 27–42. [[CrossRef](#)] [[PubMed](#)]

3. Kelemen, L.E. The role of folate receptor alpha in cancer development, progression and treatment: Cause, consequence or innocent bystander? *Int. J. Cancer* **2006**, *119*, 243–250. [[CrossRef](#)] [[PubMed](#)]
4. Shen, J.; Hu, Y.; Putt, K.S.; Singhal, S.; Han, H.; Visscher, D.W.; Murphy, L.M.; Low, P.S. Assessment of folate receptor alpha and beta expression in selection of lung and pancreatic cancer patients for receptor targeted therapies. *Oncotarget* **2018**, *9*, 4485–4495. [[CrossRef](#)]
5. Zwicke, G.L.; Mansoori, G.A.; Jeffery, C.J. Utilizing the folate receptor for active targeting of cancer nanotherapeutics. *Nano Rev.* **2012**, *3*, 18496. [[CrossRef](#)]
6. Kalaydina, R.V.; Bajwa, K.; Qorri, B.; Decarlo, A.; Szewczuk, M.R. Recent advances in “smart” delivery systems for extended drug release in cancer therapy. *Int. J. Nanomed.* **2018**, *13*, 4727–4745. [[CrossRef](#)]
7. Li, X.; Szewczuk, M.R.; Malardier-Jugroot, C. Folic acid-conjugated amphiphilic alternating copolymer as a new active tumor targeting drug delivery platform. *Drug Des. Dev. Ther.* **2016**, *10*, 4101–4110. [[CrossRef](#)]
8. Li, X.; Sambhi, M.; DeCarlo, A.; Burov, S.V.; Akasov, R.; Markvicheva, E.; Malardier-Jugroot, C.; Szewczuk, M.R. Functionalized Folic Acid-Conjugated Amphiphilic Alternating Copolymer Actively Targets 3D Multicellular Tumour Spheroids and Delivers the Hydrophobic Drug to the Inner Core. *Nanomaterials* **2018**, *8*, 588. [[CrossRef](#)]
9. Li, X.; McTaggart, M.; Malardier-Jugroot, C. Synthesis and characterization of a pH responsive folic acid functionalized polymeric drug delivery system. *Biophys. Chem.* **2016**, *214–215*, 17–26. [[CrossRef](#)]
10. Sambhi, M.; Qorri, B.; Malardier-Jugroot, C.; Szewczuk, M. Advancements in Polymer Science: ‘Smart’ Drug Delivery Systems for the Treatment of Cancer. *MOJ Polym. Sci.* **2017**, *1*, 113–118. [[CrossRef](#)]
11. Sambhi, M.; DeCarlo, A.; Malardier-Jugroot, C.; Szewczuk, M.R. Next-Generation Multimodality of Nanomedicine Therapy: Size and Structure Dependence of Folic Acid Conjugated Copolymers Actively Target Cancer Cells in Disabling Cell Division and Inducing Apoptosis. *Cancers* **2019**, *11*, 1698. [[CrossRef](#)] [[PubMed](#)]
12. Malardier-Jugroot, C.; van de Ven, T.G.M.; Cosgrove, T.; Richardson, R.M.; Whitehead, M.A. Novel Self-Assembly of Amphiphilic Copolymers into Nanotubes: Characterization by Small-Angle Neutron Scattering. *Langmuir* **2005**, *21*, 10179–10187. [[CrossRef](#)] [[PubMed](#)]
13. DeCarlo, A.; Malardier-Jugroot, C.; Szewczuk, M.R. Folic Acid-Functionalized Nanomedicine: Folic Acid Conjugated Copolymer and Folate Receptor Interactions Disrupt Receptor Functionality Resulting in Dual Therapeutic Anti-Cancer Potential in Breast and Prostate Cancer. *Bioconj. Chem.* **2021**, *32*, 512–522. [[CrossRef](#)] [[PubMed](#)]
14. Hülsmeier, A.J.; Welti, M.; Hennet, T. Glycoprotein maturation and the UPR. *Methods Enzymol.* **2011**, *491*, 163–182. [[CrossRef](#)]
15. Gocheva, G.; Ivanova, N.; Iliev, S.; Petrova, J.; Madjarova, G.; Ivanova, A. Characteristics of a Folate Receptor- α Anchored into a Multilipid Bilayer Obtained from Atomistic Molecular Dynamics Simulations. *J. Chem. Theory Comput.* **2020**, *16*, 749–764. [[CrossRef](#)]
16. Amith, S.R.; Jayanth, P.; Franchuk, S.; Finlay, T.; Seyrantep, V.; Beyaert, R.; Pshezhetsky, A.V.; Szewczuk, M.R. Neu1 desialylation of sialyl alpha-2,3-linked beta-galactosyl residues of TOLL-like receptor 4 is essential for receptor activation and cellular signaling. *Cell. Signal.* **2010**, *22*, 314–324. [[CrossRef](#)]
17. Geisler, C.; Jarvis, D.L. Letter to the Glyco-Forum: Effective glycoanalysis with Maackia amurensis lectins requires a clear understanding of their binding specificities. *Glycobiology* **2011**, *21*, 988–993. [[CrossRef](#)]
18. dos-Santos, P.B.; Zanetti, J.S.; Vieira-de-Mello, G.S.; Rêgo, M.B.; Ribeiro-Silva, A.A.; Beltrão, E.I. Lectin histochemistry reveals SNA as a prognostic carbohydrate-dependent probe for invasive ductal carcinoma of the breast: A clinicopathological and immunohistochemical auxiliary tool. *Int. J. Clin. Exp. Pathol.* **2014**, *7*, 2337–2349.
19. Goldstein, I.J.; Winter, H.C.; Poretz, R.D. Chapter 12—Plant lectins: Tools for the study of complex carbohydrates. In *New Comprehensive Biochemistry*; Montreuil, J., Vliegenthart, J.F.G., Schachter, H., Eds.; Elsevier: Amsterdam, The Netherlands, 1997; Volume 29, pp. 403–474.
20. Van Damme, E.J.; Peumans, W.J.; Pusztai, A.; Bardocz, S. *Handbook of Plant Lectins: Properties and Biomedical Applications*; John Wiley & Sons: New York, NY, USA, 1998.
21. Lee, J.B.; Pyo, K.-H.; Kim, H.R. Role and Function of O-GlcNAcylation in Cancer. *Cancers* **2021**, *13*, 5365. [[CrossRef](#)]
22. Antony, A.C.; Utle, C.; Van Horne, K.C.; Kolhouse, J.F. Isolation and characterization of a folate receptor from human placenta. *J. Biol. Chem.* **1981**, *256*, 9684–9692. [[CrossRef](#)]
23. Gilmour, A.M.; Abdulkhalek, S.; Cheng, T.S.W.; Alghamdi, F.; Jayanth, P.; O’Shea, L.K.; Geen, O.; Arvizu, L.A.; Szewczuk, M.R. A novel epidermal growth factor receptor-signaling platform and its targeted translation in pancreatic cancer. *Cell. Signal.* **2013**, *25*, 2587–2603. [[CrossRef](#)] [[PubMed](#)]
24. Johnson, L.V.; Hageman, G.S. Enzymatic characterization of peanut agglutinin-binding components in the retinal interphotoreceptor matrix. *Exp. Eye Res.* **1987**, *44*, 553–565. [[CrossRef](#)] [[PubMed](#)]
25. McTaggart, M.; Malardier-Jugroot, C.; Jugroot, M. Self-assembled biomimetic nanoreactors I: Polymeric template. *Chem. Phys. Lett.* **2015**, *636*, 216–220. [[CrossRef](#)]

26. Wiegandt, H. Chapter 3—Gangliosides. In *New Comprehensive Biochemistry*; Wiegandt, H., Ed.; Elsevier: Amsterdam, The Netherlands, 1985; Volume 10, pp. 199–260.
27. Kuo, Y.-C.; Chang, Y.-H.; Rajesh, R. Targeted delivery of etoposide, carmustine and doxorubicin to human glioblastoma cells using methoxy poly(ethylene glycol)-poly(ϵ -caprolactone) nanoparticles conjugated with wheat germ agglutinin and folic acid. *Mater. Sci. Eng. C* **2019**, *96*, 114–128. [[CrossRef](#)]

Disclaimer/Publisher’s Note: The statements, opinions and data contained in all publications are solely those of the individual author(s) and contributor(s) and not of MDPI and/or the editor(s). MDPI and/or the editor(s) disclaim responsibility for any injury to people or property resulting from any ideas, methods, instructions or products referred to in the content.